doi:10.1006/jmbi.2001.5427 available online at http://www.idealibrary.com on IDEAL® *J. Mol. Biol.* (2002) **317**, 601–612

JMB

Exploring the Role of Alanine in the Structure of the Lac Repressor Tetramerization Domain, a Ferritin-like Alacoil

Amy Solan[1], Kiira Ratia[2] and Robert Fairman[1]*

[1]*Department of Molecular, Cell and Developmental Biology Haverford College, 370 Lancaster Ave, Haverford PA 19041, USA*

[2]*Department of Pharmaceutical Biotechnology, The University of Illinois at Chicago, 900 S. Ashland Ave., Room 3068 Chicago, IL 60607, USA*

**Corresponding author*

We are interested in the determinants that specify the structure of antiparallel coiled coils. Antiparallel coiled coils often contain alanine as an important interfacial packing residue; structures containing alanine at certain well-defined positions in the heptad-repeating unit are referred to as Alacoils. Two types have been identified, containing alanine at either the *g* position of the heptad repeating unit (defined as the *d* position in the Richardson nomenclature), referred to as a rop-like Alacoil, or the *e* position (*a* position in the Richardson nomenclature), referred to as a ferritin-like Alacoil. The Lac repressor tetramerization domain forms an antiparallel four-chain coiled coil, which falls into the second class of Alacoils based on recent crystal structures. The role of alanine in such structures has not yet been explored experimentally. We test the importance of alanine at the *e* positions on the oligomeric state and stability of the isolated coiled-coil domain of Lac repressor by testing the effect of mutations at this position. We find that mutation to leucine is tolerated and its moderately stabilizing effect is most likely a consequence of plasticity of this motif. The effects on stability of the mutations to either serine or glutamine can be largely accounted for by helix propensity differences between these residues and alanine. The ability of the helices to adjust to such mutations, while maintaining the basic fold of this coiled coil, was further tested by making the same changes at the more highly exposed *g* position. Leucine at the *g* positions also causes an increase in stability, presumably by subtle rearrangement of the helices to allow partial desolvation of this side-chain.

Keywords: four-chain antiparallel coiled coil; Alacoil; thermodynamic stability; protein structure; circular dichroism

Introduction

While significant progress has been made in understanding how the primary sequence of a protein dictates its folding and structure, much is still unknown.[1] One approach to this problem is to explore the balance of chemical forces exerted by the amino acid sequence in dictating the fold of a protein. The coiled-coil structure, a highly represented motif in nature, has proven to be an important tool for the study of protein folding and structure[2,3] and our understanding of the determinants defining the structural characteristics of this motif has led to some success in the design of coiled coils with novel structural and functional properties.[4,5]

Coiled coils typically consist of two or more right-handed α-helices wound around each other, forming a left-handed supercoil. The associated α-helices in a coiled coil interact *via* ''knobs-into-holes'' packing of the side-chains, in which a hydrophobic side-chain of one helix is inserted between several hydrophobic side-chains of an adjacent helix.[6] An α-helix contains 3.6 amino acid residues per turn, but the supercoiling of α-helices results in a repeat unit of 3.5 amino acid residues per turn, or seven per two turns; by convention the

Abbreviations used: CD, circular dichroism; FMOC, 9-fluorenylmethyloxycarbonyl; MALDI-TOF, matrix-assisted laser desorption ionization-time of flight; RP-HPLC, reversed-phase-high pressure liquid chromatography; SE, sedimentation equilibrium; TFA, trifluoroacetic acid; SROV, square root of variance.

E-mail address of the corresponding author: rfairman@haverford.edu

0022-2836/02/040601–12 $35.00/0

seven amino acid residues that comprise each heptad are designated positions *a* to *g*. Detailed studies have demonstrated that the hydrophobic effect, electrostatic interactions, and van der Waal's packing interactions all contribute to defining the characteristics of coiled coils. These chemical forces determine the oligomeric state, whether the chain is parallel or antiparallel, specific pairing interactions or heterospecificity, and stability.[7–9]

Structure determinants for parallel coiled coils are better understood than for antiparallel coiled coils. For example, the details of knobs-into-holes packing in the core have been extensively studied. Rotamer preferences of side-chains involved in layered *aa* pair and *dd* pair interactions can govern the oligomeric state and stability of parallel coiled coils.[10] The neighboring residues, at the *e* and *g* positions, also play an important role in structure determination (including stability, specificity, and oligomeric state); charged residues are favored in dimeric structures and small non-polar residues are often found in higher order oligomeric structures.[11,12]

In contrast, antiparallel structures have an added degree of complexity because the knobs-into-holes packing can be satisfied in several different helical arrangements. The major difference in the packing of hydrophobic residues here is that, rather than forming discrete layers of side-chain interactions in the core, the helices are offset with respect to one another such that side-chains take on a more interdigitated packing arrangement. Seminal work in identifying these features has been done by the Richardson laboratory[13] for four-helical coiled coils (two- and three-helical antiparallel coiled coils are much rarer). The Richardson laboratory defines a class of antiparallel coiled-coil structures, the Alacoil, in which alanine residues are over-represented in either the *g* position (*d* position in their nomenclature), representing the rop-like Alacoil, or the *e* position (*a* position in their nomenclature), describing the ferritin-like Alacoil. These alanine residues, being small and hydrophobic, allow for the rotation of two neighboring helices to bury the alanine residues, resulting in tight packing between this pair of helices. Given the inequivalence of the *e* and *g* heptad positions in Alacoils, there are significant differences in the structural details of these two subclasses, which can be observed particularly in the values of the helical offset and helix axis spacing parameters. In parallel structures, the helical offset is zero, resulting in a layered effect of residues at the core as described above; the helix axis spacings are all approximately 10 Å between each neighboring helix, thus defining a pseudo-4-fold symmetry along a vector through the centroid of the bundle and parallel to the helical axes.[10] Antiparallel coiled coils that do not have alanine at *e* or *g* positions maintain this pseudo-4-fold symmetry of the helical bundle. For the Alacoils, this pseudo-4-fold symmetry is broken and the helix axis distances are about 10 Å for the distal helices and either 7.5 Å for the proximal helices in the ferritin class or 8.5 Å for the rop class. The helical offset (defined as the distance between planes orthogonal to the helix axes centered at the C^{α} atoms of the *a* positions of the proximal helices) for the ferritin class is 0.20-0.25 heptad units and for the rop class is 0.4-0.5 heptad units. In the case of the rop class, because the translation results in a displacement equal to one helical turn, there is an approximate layering of *ad* pairs with this offset value.

Our research has focused on an understanding of the structure determinants for the four-chain antiparallel coiled coil from the tetramerization domain of Lac repressor. We had shown that Lac21, a 21-amino acid residue peptide derived from the C terminus of the Lac repressor, forms an antiparallel, tetrameric coiled coil.[14] About the same time, two crystal structures of intact Lac repressor containing the tetramerization domain were published and confirmed our model.[15,16] Examination of the structure published by the Lewis laboratory revealed that it belongs to the ferritin-class of Alacoils. The helix offsets in this structure are 0.22 heptad units and the helix axis distances are 7.5 Å and 10.5 Å. Two of the three *e* positions in each helix contain alanine. These alanine residues pack as knobs-into-holes, nestled between residues at the *a′*, *b′*, and *e′* positions of the proximal helix (Figure 1(a)). In contrast, because of the rotation of the helices required to bury the alanine residues, the *g* position residue is rotated out towards the solvent and away from the corresponding hole on the proximal helix made by residues at the *c′*, *d′*, and *g′* heptad positions (Figure 1(b)). The degree of solvation of the *e* and *g* positions in this structure should be quite different (compare Figure 1(c) and (d)), therefore mutations at these positions may have differential effects on several parameters, such as the stability and oligomeric state, of this four-chain coiled coil.

In order to test the importance of alanine at the *e* and *g* positions in defining structural determinants for this Alacoil and to test the apparent asymmetry of the *e* and *g* positions, we made a set of mutants in which the alanine residues were changed to either leucine, serine, or glutamine, thus testing the effects of polarity and size of the amino acid residues at these positions (Figure 2). Mutations were made to either *e* positions at residues 5 and 12 or *g* positions at residues 7 and 14. We did not mutate the *e* or *g* positions in the third heptad as inspection of the structure suggested that these residues do not take part in interhelical interactions. If such alanine residues are of integral structural importance, then any mutation should result in a destabilization of the Alacoil fold. However, given the known flexibility of helices in coiled coils, it is also possible that minor rearrangements of the backbone can accommodate such mutations, resulting in stabilities that are perhaps governed principally by the hydrophobic effect; our results are consistent with this hypothesis.

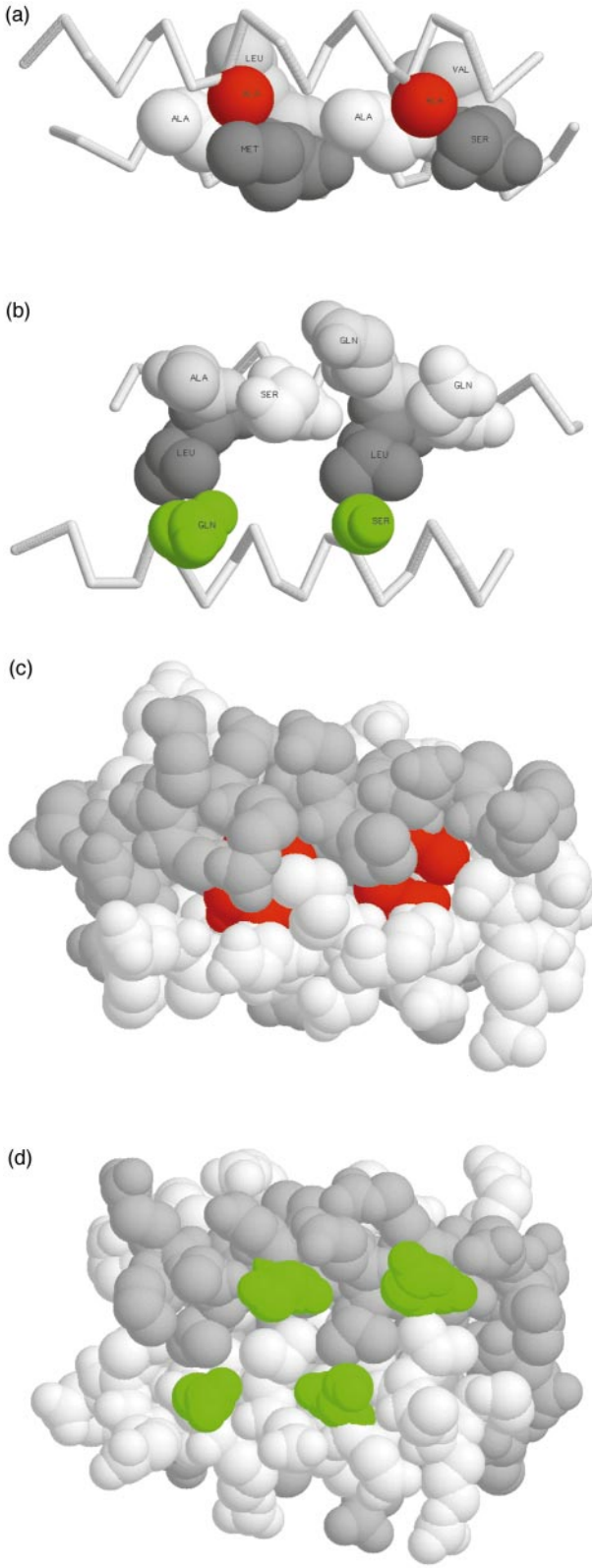

Figure 1. Space-filling models of the Lac repressor tetramerization domain comparing *e* and *g* packing interactions and degree of burial. (a) Knobs-into-holes packing of the β-carbon atoms (red) of the alanine residues at two *e* positions of one helix into two sets of residues in the proximal helix, at *a*′ (gray), *b*′ (dark gray), and *e*′ (white) positions. (b) Loss of knobs-into-holes packing of two *g* position residues, serine and glutamine (both in green) between two sets of residues in the proximal helix, at *c*′ (gray), *d*′ (dark gray), and *g*′ (white) positions. (c) Four *e* position alanine residues (red), two from each helix, at one interface of the tetramerization domain showing high degree of burial. (d) Serine and glutamine residues (both in green) at the *g* positions of two distal helices showing high degree of solvation.

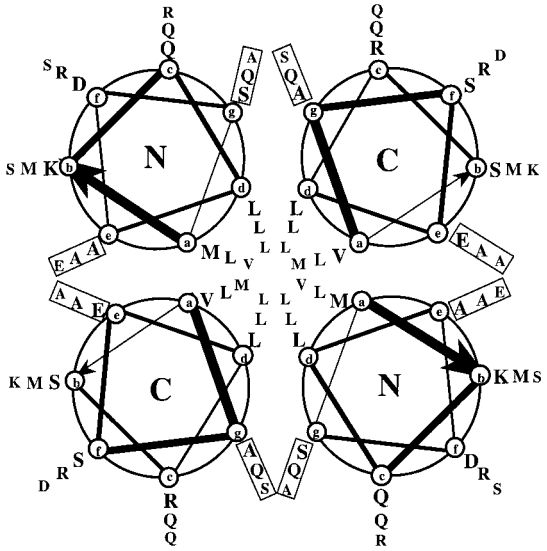

Figure 2. Four-chain coiled coil helical wheel diagram depicting the wild-type Lac21 sequence. Each large circle represents a single α-helix looking down the axis. N and C distinguish helices oriented with their amino (or carboxy) termini toward the viewer. The lower case letters in the circles represent the seven positions within each heptad unit. The upper case letters represent the residues of the Lac21 sequence in single amino acid letter code (A, alanine; D, aspartic acid; E, glutamic acid; K, lysine; L, leucine; M, methionine; Q, glutamine; R, arginine; S, serine; V, valine). The peptide sequences are:

```
                abcdefg abcdefg abcdefg
AeAe: Ac-MKQLADS LMQLARQ VSRLESA-CONH2
LeLe: Ac-MKQLLDS LMQLLRQ VSRLESA-CONH2
QeQe: Ac-MKQLQDS LMQLQRQ VSRLESA-CONH2
SeSe: Ac-MKQLSDS LMQLSRQ VSRLESA-CONH2
                abcdefg abcdefg abcdefg
AgAg: Ac-MKQLADA LMQLARA VSRLESA-CONH2
LgLg: Ac-MKQLADL LMQLARL VSRLESA-CONH2
QgQg: Ac-MKQLADQ LMQLARQ VSRLESA-CONH2
SgSg: Ac-MKQLADS LMQLARS VSRLESA-CONH2
```

.

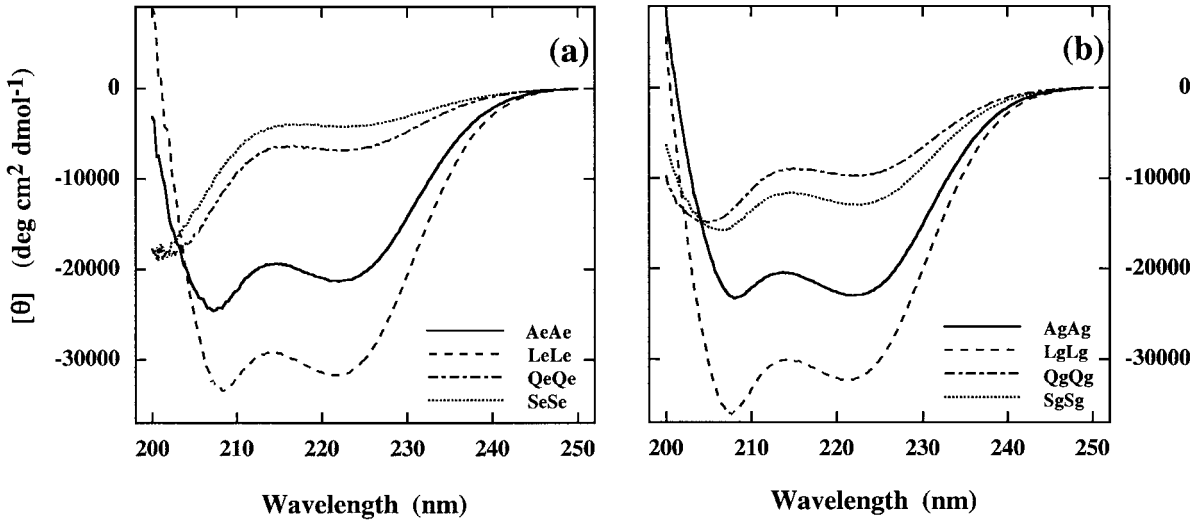

Figure 3. Circular dichroism (CD) spectra were collected at 25 °C for each mutant in 10 mM Mops (pH 7.0) and 200 μM peptide. (a) *e* mutant CD spectra. (b) *g* mutant CD spectra.

Results

Analysis of mutations at *e* positions

To test the influence of the alanine residues at the *e* positions in the first two heptads on stability and oligomerization, they were mutated simultaneously to either a non-polar residue, leucine, or to the polar residues, serine or glutamine. Synthetic peptides containing each of these mutations were assessed for their helical content and compared to a peptide containing the ''wild-type'' sequence, using circular dichroism (CD) spectropolarimetry (Figure 3(a)). The sequences and nomenclature for all the peptides used here are given in Figure 2. CD spectra were collected at the same concentration for each peptide, thus the spectra can be directly interpreted in terms of relative stabilities. CD spectra of these peptides are consistent with a secondary structure dominated by α-helices, with two minima: one in the range 200-208 nm and another at 222 nm. The spectra of SeSe and QeQe (peptides containing either serine or glutamine in place of alanine in each of two *e* positions) both exhibit a weak minimum at 222 nm and a more intense minimum around 200 nm, indicative of being largely in the unfolded state. In contrast, the LeLe spectrum has a much more intense signal at 222 nm, with a concomitant red shift in the second band to about 208 nm, indicating a high degree of helix content. The wild-type (AeAe) spectrum lies somewhere in between that seen for LeLe and both SeSe and QeQe, suggesting that, at this concentration, the peptide is in equilibrium between monomer and oligomer states.

Since the mutations that were introduced lie at the helix packing interface, and thus could influence the oligomerization state, the effects of these mutations on the oligomeric states of each of our

Table 1. Sedimentation equilibrium analysis of peptides

		SROV[a] ($\times 10^3$)					
Peptide	(conc) (μM)	Single species[b]	Monomer	Tetramer	1 ↔ 4	4 ↔ 8	1 ↔ 4 ↔ 8
AeAe,	200	4.16	30.4	4.37	4.05	4.46	3.97
LeLe,	50	5.23	49.2	21.0	21.0	4.66	4.61
	50[c]	6.11	21.2	6.10	6.06	6.09	5.39
QeQe,	100[e]	5.39	8.21	13.1	5.30	-[d]	5.30
	100[f]	4.89	7.72	8.45	5.04	-	5.04
SeSe,	200	4.99	5.06	13.0	5.32	-	5.32
AgAg,	200	3.45	14.7	5.58	5.59	3.45	3.55
LgLg,	50	3.80	28.3	7.66	7.85	4.11	4.12
	50[g]	3.94	28.7	4.32	4.37	3.84	3.68
QgQg,	200	4.65	31.6	10.6	5.22	10.6	5.23
SgSg,	200	4.02	29.9	5.24	5.26	3.68	3.24

[a] SROV is the square root of variance of the fit to the data.
[b] Single species model is calculated based on using a varying molecular weight parameter.
[c] Measured in 3.5 M urea.
[d] Dashes indicate no convergence in fitting this model.
[e] Measured in 1.5 M NaCl.
[f] Measured in 4.0 M NaCl.
[g] Measured in 6 M urea.

peptides were tested. Sedimentation equilibrium ultracentrifugation (SE) was used for this analysis (Table 1). SE analysis of 200 μM AeAe indicates that this peptide is in dynamic equilibrium between monomers and tetramers and agrees well with our previous work on Lac21, using an earlier nomenclature for the same peptide.[14] Model analysis of the SE data for the AeAe peptide is presented in Table 1. The square root of variance (SROV) is reported as a quantitative measure of the fits of various models to our data. For the AeAe peptide, as expected, a tetramer model represents a much better fit to the data than that of a monomer model (SROV of 4.37 *versus* 30.4, respectively). A moderate improvement in the fit is obtained using a two-state model with the peptide in equilibrium between monomers and tetramers. Since there is evidence for molecular weights larger than that of tetramers for some of our other peptides, tetramer-octamer and monomer-tetramer-octamer models were considered. This is not meant to suggest that the higher order states of our peptides are necessarily octameric; it is used as a convenient way to test for the presence of higher molecular weight aggregates. For the AeAe peptide, no improvement is seen in the fits to the data for models that include an octamer species. Finally, the possibility of a dimeric intermediate state for AeAe (as well as for all other peptides in this study) was considered, but no improvements in the fits were observed and thus these results are not included here.

Analytical ultracentrifugation experiments were performed for each of the other peptides at multiple concentrations and rotor speeds and sometimes in the presence of a chemical denaturant or stabilizing salt, depending on the stability of the given peptide (Table 1). Ultracentrifuge experiments for LeLe were carried out at 50 μM peptide. The best fit models for this peptide required the inclusion of a state larger than that of a tetramer. To determine if this was a consequence of an ill-determined partial specific volume or owing to higher order aggregation, we analyzed the sedimentation behavior of LeLe in the presence of 3.5 M urea (Figure 4). Urea should help reduce the level of aggregation, resulting in a lower apparent molecular weight, while having little impact on the partial specific volume of the peptide. Figure 4(a) shows global fits to data collected at three rotor speeds for either a tetramer model or a tetramer-octamer model. There is a clear improvement in the residuals from the fitting upon inclusion of an octamer state. Addition of urea results in a significant improvement in the fit using a monomer-tetramer model with no distinguishable difference between this model and a three-state monomer-tetramer-octamer model (Figure 4(b)). This result is borne out by the SROV analysis as well. A tetramer-octamer model predicts that approximately 24 % of the peptide is aggregated to states larger than the tetramer state. Since aggregation above that of a tetramer is largely eliminated by 3.5 M urea, this higher order aggregation is not likely to significantly influence the measurement of stability using urea as a denaturant as shown in Figure 8(a) for LeLe.

In contrast, the QeQe peptide is much less stable and is largely monomeric by sedimentation equilibrium as judged by the difference in SROV for monomer and tetramer models. In fact, establishing clear evidence for the tetramer in this peptide was not possible without the addition of NaCl to populate the tetramer. Addition of salt is well-known to help stabilize proteins through its effects on the hydrophobic contribution to stability and the NaCl dependence of coiled-coil stability for QeQe is shown in Figure 6(a). Therefore, SE experiments on QeQe were performed in 1.5 M and 4.0 M NaCl, representing a point midway through the folding transition and a second point in which the peptide is largely folded (Table 1). The SE results confirm that, while highly unstable, the QeQe peptide still has the structure determinants for a four-chain coiled coil. The SeSe peptide was determined also to be largely monomeric by SE and attempts to stabilize the structure through the addition of NaCl were unsuccessful owing to peptide precipitation in the time-frame of the ultracentrifuge experiments.

The stabilities of these peptides were quantified by thermal denaturation using CD as a probe. The signal at 222 nm was used to quantify helix content.[14] Thermal denaturations performed on the *e* mutants at a constant peptide concentration of 100 μM (Figure 5(a)) gave the following order of stabilities for the *e* mutants: LeLe > AeAe > QeQe ≅ SeSe, in good agreement with the qualitative conclusions reached by inspection of the CD spectra. As is often seen for coiled-coil thermal unfolding, cold denaturation is a prominent feature,[17] and is most evident in the unfolding curve for the AeAe peptide. As expected for a concentration-dependent folding reaction, increasing peptide concentration results in an increased t_m in thermal unfolding experiments, along with an apparent increase in signal intensity, as the t_m values for cold and heat denaturation diverge from one another (data not shown).

A free energy value for each of the mutants was extracted by fitting the data using the Gibbs-Helmholtz equation modified accordingly to describe the unfolding of an oligomeric system. We have justified the thermodynamic treatment of such data in our previous work on this model system.[14,18] The problem that we faced in a thermodynamic treatment here is the lack of well-defined pre- and post-transition baselines. Since the post-transition baselines are similar for the AeAe, QeQe, and SeSe peptides, it was assumed that the LeLe peptide, in which this baseline is not evident, must be the same. It is harder to make a similar assumption for a pre-transition slope since the LeLe peptide provides the only dataset with a well-defined native baseline. To test such an assumption, the weakly associating peptides were stabilized by the

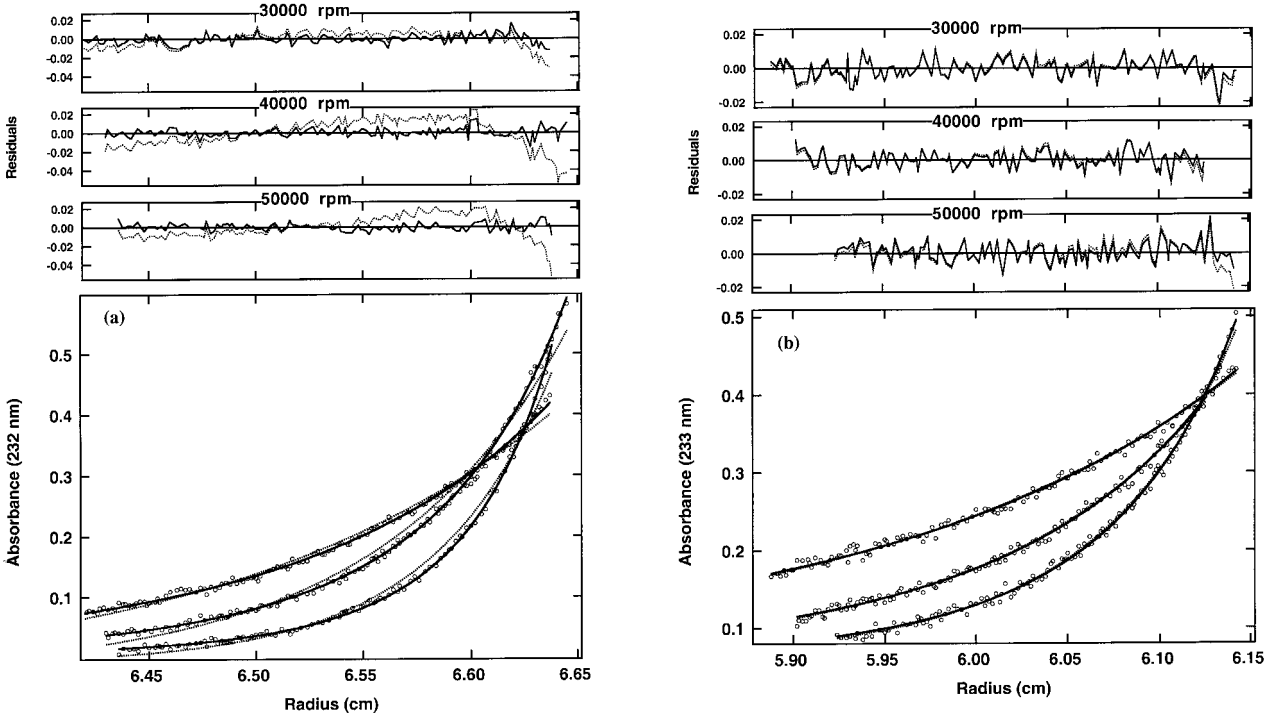

Figure 4. Sedimentation equilibrium analyses for 50 μM LeLe peptide in (a) 0 M and (b) 3.5 M urea. The data are fit globally with either a monomer-tetramer model (---) or a monomer-tetramer-octamer model (—). The residuals from the fits are shown above for each speed. Solvent densities: 0.9975 g/ml for the buffer alone and 1.0521 g/ml for the buffer plus 3.5 M urea.

addition of NaCl (Figure 6(a)) in order to establish a well-defined baseline in thermal unfolding experiments. For each of the less stable peptides, the addition of NaCl results in stabilization of the tetramer, as seen in the SE data as well, and further, the magnitude of the mean residue ellipticity of the stable tetramers is in good agreement with that of the LeLe tetramer. Thermal unfolding of AeAe, as measured in the presence of NaCl, demonstrates that the pre-transition baseline is identical to that observed for LeLe (Figure 6(b)), thus justifying the extraction of a free energy at 25 °C.

The free energies of these peptides are shown in Table 2. As we have pointed out before,[19] obtaining accurate free energies requires either that the reported free energy be within, or near, the folding transition or that there is clear evidence for cold denaturation to help establish a reasonable value for the heat capacity, in order to extrapolate a free energy outside of the transition zone. In most cases, the data here fulfill this requirement. Nevertheless, given the high stability of the LeLe peptide, the free energy extrapolated to 25 °C is ill-determined. Free energies in the range −26,000 to −36,000 cal/(mol-tetramer) can fit these data reasonably well for different fixed values of the heat capacity, ranging from 500 to an unrealistic value of −2000 cal/(mol-tetramer) per deg, when allowing for enthalpy compensation in the fitting protocol. In contrast, the fits to the data for the AeAe, QeQe, and SeSe peptides provide much more robust free energies. In a similar sensitivity

Table 2. Stabilities of the *e* and *g* mutants

Peptide	ΔG^{0a}		
	Temperature	[GuCl] (*m*) [b]	[Urea] (*m*) [a]
AeAe	−4.1 (29) [c]	−4.4 (1.3)	−4.3 (0.75)
LeLe	−7.0 (91)	−6.1 (2.3)	−5.9 (1.4)
QeQe	−3.5 (−4)	−3.5 (0.56)	−3.4 (0.72)
SeSe	−3.2 (−31)	−3.4 (0.38)	−3.3 (0.41)
AgAg	−4.6 (64)	−5.0 (1.2)	−4.9 (0.54)
LgLg	−7.6 (99)	−7.0 (2.2)	−6.5 (0.94)
QgQg	−3.7 (−9)	−3.7 (0.62)	−3.6 (0.68)
SgSg	−3.7 (−8)	−3.8 (1.0)	−3.7 (0.79)

[a] All free energies are reported in kcal/mol of monomer using a 1 M peptide standard state at 25 °C.
[b] *m* represents the [denaturant] dependence of the free energy in kcal/mole of monomer/Mol denaturant.
[c] High temperature unfolding midpoints, in deg. C, assuming no cold denaturation ($\Delta C_p = 0$).

analysis for the SeSe data, using test values of 100 and 500 cal/(mol-tetramer) per deg (the best fit value is 325 cal/mol per deg) results in significant deviations of the model from the data and only modest changes in the free energy in the range −12,880 to −12,910 cal/(mol-tetramer), respectively. This somewhat surprising result, especially for the SeSe peptide where the transition is so poorly defined, suggests that reasonably accurate free energies can be ascertained, provided that information about pre- and post-transition baselines is available.

It is well understood that extrapolation methods to quantify stability can magnify errors. Thus, the accuracy of the free energies reported from the thermal unfolding data was tested by measuring the stabilities using both guanidinium chloride and urea as denaturants. Chemical denaturations were performed on this set of mutants, at various peptide concentrations, again using CD as a probe (Figures 7(a) and 8(a)). As in the case of the thermal unfolding data, LeLe was the only peptide of sufficient stability to provide a full transition between the folded and unfolded states. Nevertheless, making similar assumptions about the pre-transition baselines in these experiments, free energies were extracted from both the chemical denaturation experiments (Table 2). Also shown in Table 2 is the dependence of the free energy on either [GuCl] or [urea] as an m value. As with the thermal unfolding data, a free energy sensitivity analysis was performed for a few representative cases (LeLe, AeAe, and SeSe) using the urea denaturations. The LeLe data provide a good basis set to extract a rigorous free energy. The m value for the LeLe peptide is 1440 cal/(mol-tetramer) per (M-urea) and variation of $> \pm 300$ about this value reveals significant non-randomness in the fit. This error range represents deviations in the free energy from the value of −23,400 cal/(mol-tetramer) of ±900. Similar sensitivity analyses of the data for the AeAe and SeSe peptides provide uncertainties of approximately ±300 cal/(mol-tetramer) for both.

The free energies, as measured by these different experiments, are in fairly good agreement with one another, thus justifying such a treatment of truncated data sets. The largest discrepancies are in the apparent over-prediction of the stability for LeLe by thermal denaturation; this is most likely explained by the ill-determined nature of the free energy owing to the enthalpy-heat capacity compensation problem as discussed above. Overall, the differences in free energies upon mutation are quite small. The largest difference is the mutation to leucine, giving a $\Delta\Delta G$ in the range of −800 to −1500 cal/mol per residue, a value that is significantly smaller than that expected for the difference in the desolvation of alanine *versus* leucine, which has been calculated to be −1900 cal/mol.[20]

Analysis of mutations at *g* positions

Since the leucine is readily accommodated in an apparently sterically constrained environment in the *e* heptad position, even resulting in a modest increase in coiled-coil stability, the helices obviously are sufficiently plastic to adjust to the increased volume of this residue; such a result was predicted by Gernert *et al*.[13] In order to further test the plasticity of this motif, these same mutations were engineered into two *g* heptad positions. In addition, to provide consistency in the approach to our thermodynamic analysis, a reference peptide was made in which the native residues at the *g* positions had been replaced with alanine. Thus, $\Delta\Delta G$s for the *g* mutations are reported relative to this reference peptide. The CD spectra (Figure 3(b)), thermal unfolding curves (Figure 5(b)), and chemical denaturation curves (Figures 7(b) and 8(b)) for the *g* mutant peptides show that the order of stabilities parallel the order observed for the *e* mutants, but in general are more stable than their *e* mutant counterparts. For example, the CD spectra for SgSg and QgQg appear to be partially helical, in contrast to that observed for SeSe and QeQe. The thermodynamic parameters from these experiments are shown in Table 2. The general increase in the stability of each of the *g* mutants, relative to their *e* mutant counterparts, can be largely explained by the difference in helix propensities between the two reference peptides (see Discussion). In AeAe, the *e* and *g* positions in the first two heptads of each peptide collectively contain two alanine residues, a serine, and a glutamine, whereas in AgAg, all four residues are alanine. Thus, the difference in stabilities can be accounted for by the difference in helix propensities of substituting a serine and glutamine with two alanine residues (Table 3). It is interesting to note that the mutation to leucine at either the *e* or *g* positions results in a similar change in free energy, indicating that the helices can similarly accommodate the partial desolvation of these side-chains (Table 3).

Results of SE analysis of the *g* mutants also largely parallel those for the *e* mutants. Like the LeLe peptide, the LgLg peptide shows evidence for some aggregation above that of a tetramer. Again, addition of urea helps to alleviate this aggregation. Given the increased stabilities of the QgQg and SgSg peptides, relative to their *e* counterparts, it was more straightforward to establish the oligomeric states from the SE analysis. In all cases, a monomer-tetramer equilibrium model fits well to the data.

Discussion

The importance of alanine residues in specifying structural features of the Alacoil subclass of antiparallel coiled-coil structures was investigated.[13] Analysis of the Lac repressor tetramerization domain identifies it as a member of the ferritin-like Alacoil. In order to explore the structural role of

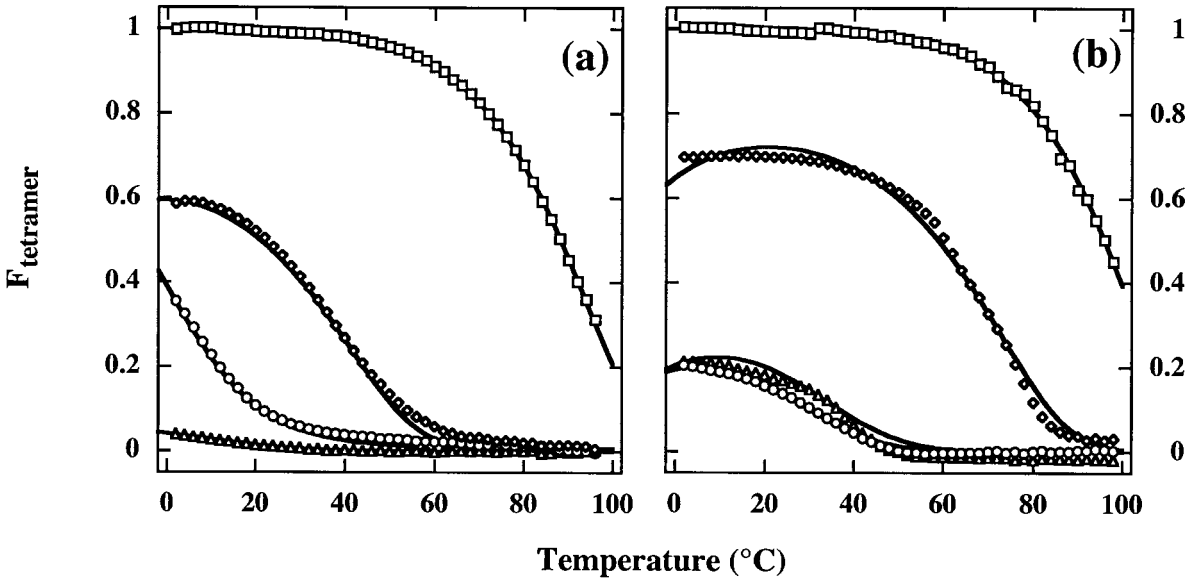

Figure 5. CD thermal unfolding experiments for (a) the *e* mutants: LeLe (squares), AeAe (diamonds), QeQe (circles), and SeSe (triangles) and (b) the *g* mutants: LgLg (squares), AgAg (diamonds), QgQg (circles), and SgSg (triangles). All experiments were performed using 100 μM peptide in 10 mM Mops (pH 7.0).

alanine, the oligomeric states and stabilities of a series of peptides were studied containing mutations at *e* or *g* heptad positions. All of the peptides studied here maintained their specificity determinants for tetramer formation as determined by SE experiments indicating that, in the context of the Lac repressor sequence, the alanine residues do not play an influential role in this structural feature (Table 1). Additionally, such mutations have at best a moderate affect on the stability of this motif, as judged by the thermodynamic analysis presented in Table 2.

In general, replacing the alanine residues that define the Alacoil with leucine is significantly stabilizing as predicted by Gernert *et al.*[13] Mutations to leucine in the *g* heptad positions also result in added stability, suggesting that the effect is due to a general increase in the burial of hydrophobic surface area rather than in specific packing effects. In fact, placement of leucine residues at *e* and *g* positions was an important element of early design efforts for antiparallel helical bundles.[21]

Replacement of the alanine residues with either serine or glutamine results in an apparent decrease in stability. However, this decrease in stability, as measured at the *e* heptad positions, can be accounted for through the change in helix propensity upon mutation from alanine to the appropriate

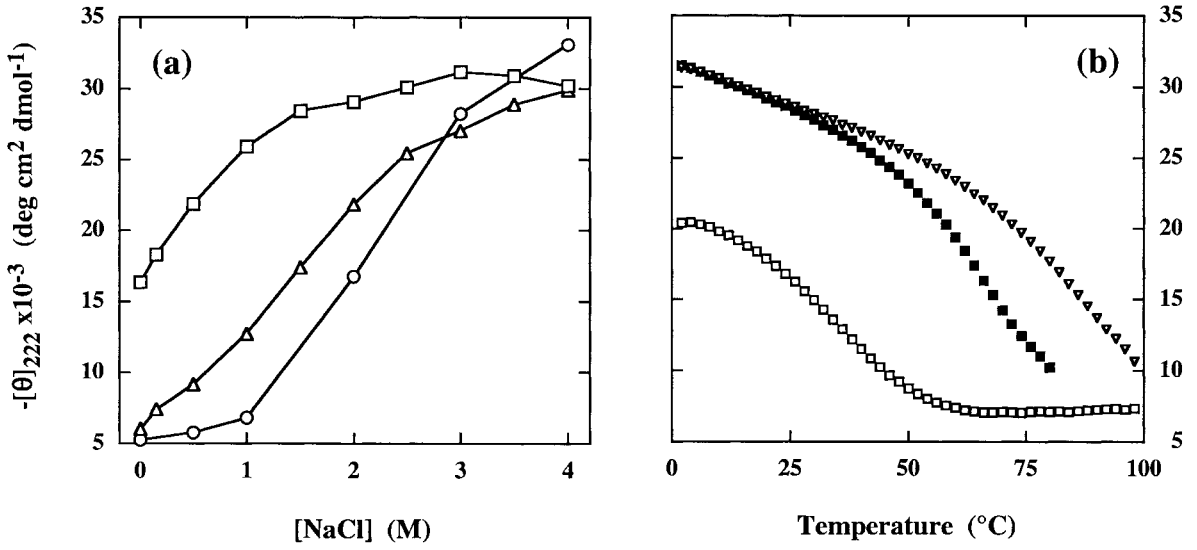

Figure 6. (a) [NaCl] dependence of stability for AeAe (squares), QeQe (triangles), and SeSe (circles). (b) Thermal unfolding of AeAe in 2 M NaCl (filled squares) as compared to AeAe (open squares) and LeLe (triangles) without NaCl.

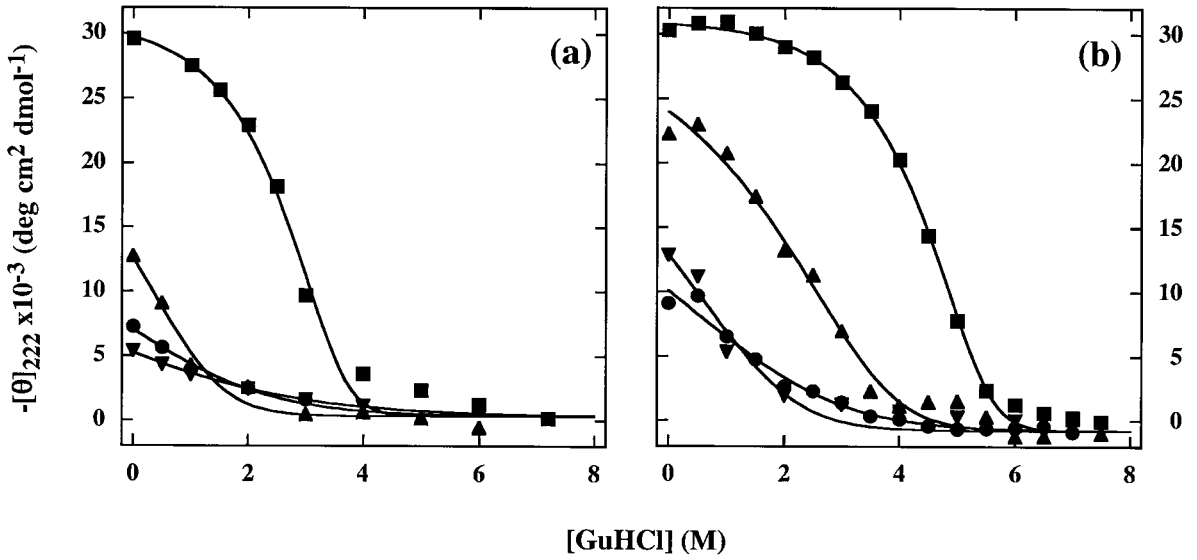

Figure 7. GuHCl denaturations were performed on each mutant in 10 mM Mops (pH 7.0). (a) *e* mutant denaturations using the following concentration of peptide: 50 μM LeLe (squares), 50 μM AeAe (triangles), 200 μM QeQe (circles), and 200 μM SeSe (inverted triangles). (b) *g* mutant denaturation using the following concentration of peptide: 50 μM LgLg (squares), 50 μM AgAg (triangles), 200 μM QgQg (circles), and 200 μM SgSg (inverted triangles).

residue (Table 3). Helix propensity corrections have been used in the past to determine the impact of side-chain interactions on coiled coil stability [18,19] using a helix propensity free energy scale measured for a coiled coil system as a basis set.[22] The helix propensity of leucine is unfavorable relative to alanine, and thus correction for the difference in helix propensities leads to a larger free energy associated with burial of the leucine side-chain relative to alanine. For example, considering the urea denaturation data for LeLe, the difference in free energy from the reference peptide, AeAe, is −1600 cal/(mol-monomer) but upon inclusion of a propensity penalty of +380 cal/(mol-monomer), the overall effect of the two leucine replacements is −2000 cal/(mol-monomer), or −1000 cal/mol for each alanine-leucine mutation. In contrast, for QeQe and SeSe, all of the destabilizing effect of the mutated residues can be ascribed to helix propensity effects as the difference in free energies is close to zero. Replacement of alanine with glutamine or serine at the *g* heptad positions is somewhat more destabilizing than predicted from differences in helix propensities. This is a puzzling result as,

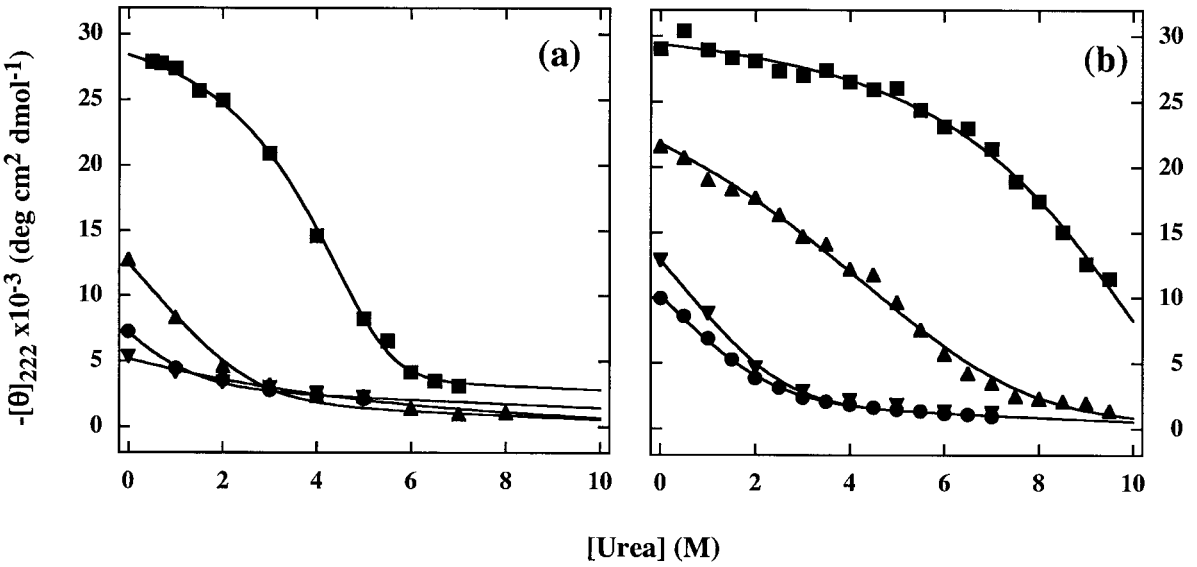

Figure 8. Urea denaturations were performed on each mutant in 10 mM Mops (pH 7.0) at the same peptide concentrations as reported in Figure 7. (a) *e* mutant denaturations: LeLe (squares), AeAe (triangles), QeQe (circles), SeSe (inverted triangles); (b) *g* mutant denaturations: LgLg (squares), AgAg (triangles), QgQg (circles), SgSg (inverted triangles).

Table 3. $\Delta\Delta G^{\circ}$s corrected by helix propensity differences

Peptide	ΔG^{0}[a] based on urea denaturation	$\Delta\Delta G^{0}$[b]	Propensity penalty[c]	Residual interaction
AeAe	−4.3	-	-	-
LeLe	−5.9	−1.6	+0.38	−2.0
QeQe	−3.4	+0.9	+0.76	+0.14
SeSe	−3.3	+1.0	+0.88	+0.12
AgAg	−4.9	-	-	-
LgLg	−6.5	−1.6	+0.38	−2.0
QgQg	−3.6	+1.3	+0.76	+0.54
SgSg	−3.7	+1.2	+0.88	+0.32

[a] All free energies are reported in kcal/mol of monomer using a 1 M standard state at 25 °C.
[b] Difference between AeAe or AgAg and peptide of interest.
[c] Helix propensities are calculated using data from Betz *et al.*[22] based on dimeric and trimeric coiled coil systems.

given that residues at this position of the Alacoil are more highly solvated, it would be predicted that these mutations would have an even more benign effect on stability compared to the same mutations at the *e* heptad positions.

We applied energy minimization routines, using the Discover module of Insight95, to see how the helices might adjust to the mutations introduced at the *e* positions. The sequences used here were built starting with the structure reported from Lewis' laboratory (1LBI).[15] We found that the mutation of the *e* position alanine residues to leucine resulted in improved energies as a consequence of significant changes in the juxtaposition of the helices with respect to one another. The proximal helices rotate to provide increased van der Waal's contact between the introduced leucine residues and then move apart to accommodate the increased side-chain volume such that the distances between the helical axes are more similar to that seen in parallel helical bundles, with uniform helix axis distances on the order of 10 Å. In contrast, the mutations to serine residues did not significantly affect the structure or energies after minimization. This is not unexpected since serine can often replace alanine in helices because burial of the hydroxyl group can be compensated by the formation of an H-bond with the backbone.[23] The placement of the serine hydroxyl group in the minimized structure is consistent with the possibility of forming such H-bonds. While no conclusive results were obtained for the mutations to glutamine, it is clear that these mutations did not have a significant impact on the minimized structure or energies. While these modeling studies should not be interpreted quantitatively in terms of comparing the stabilities to the experimentally determined values, it is intriguing to note that the helices readily adjust away from the Alacoil geometry to the more canonical geometry of an anti-parallel four-helix bundle.

Thus, the *e* position alanine residues in the antiparallel coiled coil from Lac repressor do not play a dominant role in determining the oligomeric state and are of only minor importance as stability determinants. It can tentatively be concluded that the role of alanine in this structure is as a specificity determinant, influencing the precise geometry of the coiled-coil structure. It is not obvious why specifying such a structure might be of importance to the function of the Lac repressor protein. Our results from our leucine mutations are similar to that seen for the sequences studied by the DeGrado laboratory who have shown that such sequences are dynamic and have many characteristics of a molten globule.[24] In light of the albeit indirect evidence for increased dynamics in the leucine mutants, it is likely that the details of the geometry and packing interactions for the leucine mutants (and possibly the glutamine mutants) are quite different from that of the Alacoils. Further work on similar Alacoils will be important to elucidate the influence of this subclass of antiparallel coiled coils on the functions of proteins that contain this motif.

Materials and Methods

Peptide synthesis and purification

The synthesis and purification of the *e* and *g* mutant peptides were carried out as described by Vu *et al.*[19] All peptides were synthesized manually using standard FMOC chemistry and using PAL resin (Advanced ChemTech), which provides an amide at the carboxy-terminal end upon TFA cleavage. The peptides were acetylated at the amino terminus prior to TFA cleavage. The peptides were purified by reversed-phase HPLC and the identities of the products were verified by MALDI-TOF mass spectrometry. Stock solutions of peptides were prepared by lyophilization and dissolution in Milli-Q purified water to about 1-2 mM concentration. Concentration of the peptide solutions was determined by a modified ninhydrin assay[25] and by amino acid analysis when inconsistent results were obtained by the ninhydrin method.

Circular dichroism spectropolarimetry

CD data were collected on an Aviv 62A circular dichroism spectropolarimeter. All CD samples were prepared in 10 mM Mops (pH 7.0), and measurements were taken using a bandwidth of 1.5 nm. Spectra were collected from 195 to 250 nm at 25 °C, with a step size of 0.25 nm and an averaging time of two seconds. Thermal denaturations were collected from 2 to 98 °C at 222 nm, with a step size of 2 nm and 25 °C. Algorithms encoded using MLAB[25] were used to fit the thermal denaturation

data and the urea and GuHCl denaturation data and allowed for the calculation of free energy values for the mutants.[17] Stabilities were quantified by fitting thermal unfolding experiments using the Gibbs-Helmholtz function to define the temperature dependence of a monomer-tetramer equilibrium.[17]

Pre-transition and post-transition baselines were fitted as described by Vu *et al*.[19] Justification for fixed slope and intercept values for the pre-transition baselines for all the peptides was based on measuring the CD signal under conditions where 100% helix formation is expected using NaCl to induce this effect. Addition of NaCl in thermal unfolding experiments using the AeAe peptide as a test case (Figure 7(a)), was done to demonstrate that the pre-transition slope for highly unstable peptides is the same for related coiled coil peptide systems.

Analytical ultracentrifugation

Sedimentation equilibrium experiments were performed at 25 °C in a Beckman model XLA analytical ultracentrifuge using an An 60 Ti rotor. Data were collected using six-channel Epon, charcoal-filled centerpieces with 12-mm pathlengths containing 110 μl samples and 125 μl buffer references. Samples in 10 mM Mops (pH 7.0) were centrifuged at 30,000, 40,000, and 50,000 rpm. The sedimentation equilibrium data were analyzed using either the HID program from the Analytical Ultracentrifugation Facility at the University of Connecticut or an SE curve-fitting algorithm running in Igor PPC 3.16. Temperature-corrected partial specific volumes (LeLe: 0.7559 ml/g, SeSe: 0.7331 ml/g, QeQe: 0.7338 ml/g, LgLg: 0.7642 ml/g, AgAg: 0.7493 ml/g, SgSg: 0.7409 ml/g, QgQg: 0.7413 ml/g) were calculated from the weight average of the partial specific volumes of the individual amino acids.[27] Densities for the different solution conditions were also calculated using tables from Laue *et al*.[27]

Molecular modeling

The starting model for energy minimizations was the structure of the tetramerization domain from Lac repressor[15] modified in the following manner using the Biopolymer module running in InsightII 97 (Biosym Technologies, San Diego). The amino-terminal residues that define the start of the coiled-coil domain, containing proline, arginine, and alanine, were mutated to methionine, lysine, and glutamine, to be consistent with the design of the peptides used in this study and in our previous work.[14,18,19] Also, serine and alanine were appended to the C-terminal glutamic acid in a helical conformation. Side-chains were manually adjusted to the most energetically favorable rotamer and molecular mechanics were run in Discover using a combination of steepest descents and conjugate gradients to optimize the modified structure. Mutations were then introduced to this structure at each of the *e* positions in the first two heptads. Further minimization was applied to accommodate these new residues, using 800 iterations of steepest descents and 10,000 iterations of conjugate gradients.

Acknowledgements

We thank Jim Robblee for his help with analytical ultracentrifugation, Jim Lear for the Igor algorithms for data analysis, Lawrence Lee for peptide purification, Ben North for Lac repressor coiled coil parameterization, and Bill DeGrado for the use of his MALDI-TOF spectrometer. We also thank Lina Dahlberg and Annette Pasternak for editorial comments. We gratefully acknowledge support from NSF MCB-9817188 and NSF DBI-9970203 grants.

References

1. Radford, S. (2000). Protein folding: progress made and promises ahead. *Trends Biochem. Sci.* **25**, 611-618.
2. Burkhard, P., Stetefeld, J. & Strelkov, S. V. (2001). Coiled coils: a highly versatile protein folding motif. *Trends Cell Biol.* **11**, 82-88.
3. Lupas, A. (1996). Coiled coils: new structures and new functions. *Trends Biochem. Sci.* **21**, 375-382.
4. Micklatcher, C. & Chmielewski, J. (1999). Helical peptide and protein design. *Curr. Opin. Chem. Biol.* **3**, 724-729.
5. Bryson, J. W., Betz, S. F., Lu, H. S., Suich, D. J., Zhou, H. X., O'Neil, K. T. & DeGrado, W. F. (1995). Protein design: a hierarchic approach. *Science,* **270**, 935-941.
6. Crick, F. H. C. (1953). The packing of α-helices: simple coiled coils. *Acta Crystallog.* **6**, 689-697.
7. Cohen, C. & Parry, D. A. D. (1990). α-Helical coiled coils and bundles: how to design an α-helical protein. *Proteins: Struct. Funct. Genet.* **7**, 1-15.
8. Hodges, R. S. (1992). Unzipping the secrets of coiled-coils. *Curr. Biol.* **2**, 122-124.
9. Cohen, C. & Parry, D. A. D. (1994). α-Helical coiled coils: more facts and better predictions. *Science,* **263**, 488-489.
10. Harbury, P. B., Zhang, T., Kim, P. S. & Alber, T. (1993). A switch between two-, three-, and four-stranded coiled coils in GCN4 leucine zipper mutants. *Science,* **262**, 1401-1407.
11. Baxevanis, A. D. & Vinson, C. R. (1993). Interactions of coiled coils in transcription factors: where is the specificity? *Curr. Opin. Genet. Dev.* **3**, 278-285.
12. Krylov, D., Mikhailenko, I. & Vinson, C. R. (1994). A thermodynamic scale for leucine zipper stability and dimerization specificity: e and g interhelical interactions. *EMBO J.* **13**, 2849-2861.
13. Gernert, K. M., Surles, M. C., LaBean, T. H., Richardson, J. S. & Richardson, D. C. (1995). The Alacoil: a very tight, antiparallel coiled-coil of helices. *Protein Sci.* **4**, 2252-2260.
14. Fairman, R., Chao, H. G., Mueller, L., Lavoie, T. B., Shen, L., Novotny, J. & Matsueda, G. R. (1995). Characterization of a new four-chain coiled-coil: influence of chain length on stability. *Protein Sci.* **4**, 1457-1469.
15. Lewis, M., Chang, G., Horton, N. C., Kercher, M. A., Pace, H. C., Schumacher, M. A. *et al*. (1996). Crystal structure of the lactose operon repressor and its complexes with DNA and inducer. *Science,* **271**, 1247-1254.
16. Friedman, A. M., Fischmann, T. O. & Steitz, T. A. (1995). Crystal structure of *lac* repressor core tetra-

mer and its implications for DNA looping. *Science,* **268**, 1721-1727.
17. Boice, J., Dieckmann, G., DeGrado, W. & Fairman, R. (1996). Thermodynamic analysis of a designed three-stranded coiled coil. *Biochemistry,* **35**, 14480-14485.
18. Fairman, R., Chao, H. G., Lavoie, T. B., Villafranca, J. J., Matsueda, G. R. & Novotny, J. (1996). Design of heterotetrameric coiled coils: evidence for increased stabilization by Glu^{-}-Lys^{+} ion pair interactions. *Biochemistry,* **35**, 2824-2829.
19. Vu, C., Robblee, J., Werner, K. M. & Fairman, R. (2001). Effects of charged amino acids at *b* and *c* heptad positions on specificity and stability of four-chain coiled coils. *Protein Sci.* **10**, 631-637.
20. Eisenberg, D. & McLachlan, A. D. (1986). Solvation energy in protein folding and binding. *Nature,* **319**, 199-203.
21. Ho, S. P. & DeGrado, W. F. (1987). Design of a 4-helix bundle protein: synthesis of peptides which self-associate into a helical protein. *J. Am. Chem. Soc.* **109**, 6751-6758.
22. Betz, S., Fairman, R., O'Neil, K., Lear, J. & DeGrado, W. (1995). Design of two-stranded and three-stranded coiled-coil peptides. *Phil. Trans. Roy. Soc. London, Ser. B,* **348**, 81-88.
23. Vijayakumar, M., Qian, H. & Zhou, H.-X. (1999). Hydrogen bonds between short polar side-chains and peptide backbone: prevalence in proteins and effects on helix-forming propensities. *Proteins: Struct. Funct. Genet.* **34**, 497-507.
24. Handel, T. M., Williams, S. A. & DeGrado, W. F. (1993). Metal ion-dependent modulation of the dynamics of a designed protein. *Science,* **261**, 879-885.
25. Rosen, H. (1957). A modified ninhydrin colorimetric analysis for amino acids. *Arch. Biochem. Biophys.* **67**, 10-15.
26. Knott, G. D. (1979). MLAB-a mathematical modeling tool. *Comput. Programs Biomed.* **10**, 271-280.
27. Laue, T. M., Shah, B. D., Ridgeway, T. M. & Pelletier, S. L. (1992). Computer-aided interpretation of analytical sedimentation data for proteins. In *Analytical Ultracentrifugation in Biochemistry and Polymer Science* (Harding, S. E., Rowe, A. J. & Horton, J. C., eds), pp. 90-125, The Royal Society of Chemistry, Cambridge, UK.

Edited by P. E. Wright

(Received 24 August 2001; received in revised form 8 January 2002; accepted 14 January 2002)